Simultaneous Estimation of Optical Flow and Its Boundaries based on the Dynamical System Model

Yuya Michishita, Noboru Sebe, Shuichi Enokida and Eitaku Nobuyama
Kyushu Institute of Technology, Iizuka, Fukuoka, Japan

Keywords: Optical Flow, Optical Flow Boundaries, Dynamical System Model.

Abstract: Optical flow is a velocity vector which represents the motion of objects in video images. Optical flow estimation is difficult in the neighborhood of flow boundary. To resolve this problem, Sasagawa (2014) proposes a modified dynamical system model in which one assumes that, in the neighborhood of flow boundaries, the brightness flows in the perpendicular direction, and considers the resulting corrections to the brightness constancy constraint. However, in that model, the correction is occurred even in place where the flow is continuous. We propose a new model, which switches the conventional model and the proposed model in Sasagawa (2014). As a result, we expect improvement of the estimate accuracy in place where the flow is continuous. We conduct numerical experiments to investigate the improvements that the proposed model yields in the estimation accuracy of optical flows.

1 INTRODUCTION

Optical flow is a velocity vector which represents the motion of objects in video images. The estimation of optical flow is a fundamental tool for the object motion measurements using a visual sensor, and is utilized in various fields. Recently, high-accurate estimation method of optical flow has been expected to improve the performance of various video image analysis systems. Actually, the accurate boundaries information of optical flow will contribute to establish accurate estimation of the optical flow, and vice versa. However, it is a chicken and egg dilemma. In this paper, a new estimation method which has the capability of simultaneous estimation of the optical flow and its boundary is proposed.

The optical flow equation describes the brightness constancy constraint and has been used to determine optical flows in Horn and Schunck (1981) and Lucas and Kanade (1981). Sebe *et al*. (2009) is one of the optical flow estimation methods which utilize the optical flow equation. Sebe *et al*. (2009) regard the optical flow equation as a dynamical system and apply Kalman filter to that dynamical system to estimate the optical flow. Based on the method in Sebe *et al*. (2009), an estimation method was proposed to estimate dense optical flow (Fukami *et al*., 2011). There are mainly two advantages of the use of Kalman filter for dense optical flow estimation. One is that it allows us to obtain the covariance matrix of the estimation error. The covariance matrix of the estimation error provides a confidence of estimated optical flow. This enables us to assess the results of optical flow estimation, even if the actual values are not available in practice. The other advantage is that the measurement residual, which can be obtained as the difference between the estimated intensity and the measured intensity, can detect the optical flow boundary. At the boundary of optical flow, the brightness constancy constraint does not hold. In other words, the dynamical system model used for estimation is not correct. This causes a large measurement residual. Accordingly, measurement residual enables us to detect the boundary of optical flow. However, in Fukami *et al*. (2011), the boundary information of optical flow is not used to improve the accuracy of estimation.

One difficulty in optical flow estimation is that the estimation accuracy deteriorates near flow boundaries, such as occlusion. To resolve this problem, Sasagawa (2014) proposes a modified dynamical system model in which the brightness conserved quantity flows in the perpendicular direction in the neighborhood of flow boundaries. He also considers the resulting corrections to the brightness constancy constraint. The model proposed in Sasagawa (2014) improved estimation accuracy in the neighborhood of flow boundaries. However, as Sasagawa (2014) did not use any information about the measurement resid-

Michishita Y., Sebe N., Enokida S. and Nobuyama E.
Simultaneous Estimation of Optical Flow and Its Boundaries based on the Dynamical System Model.
DOI: 10.5220/0006101303770385
In *Proceedings of the 12th International Joint Conference on Computer Vision, Imaging and Computer Graphics Theory and Applications (VISIGRAPP 2017)*, pages 377-385
ISBN: 978-989-758-227-1

ual, the brightness corrections arose even in places where the flow was continuous. This deteriorate the estimation accuracy in regions not near image boundaries.

To address this difficulty, we propose a new model in which measurement residuals are used to switch between the model proposed in Sasagawa (2014) and conventional models. In our proposed model, we assume that boundaries are present in regions with large measurement residuals, and thus apply the corrections in such regions; in regions where measurement residuals are small we do not apply the corrections. Consequently, no corrections arise in regions where boundaries do not exist, whereupon we expect improved estimation accuracy. We conduct numerical experiments to investigate the improvements that the proposed model yields in the estimation accuracy of optical flows.

2 DYNAMICAL-SYSTEM-BASED ESTIMATION MODEL

In this section, following the conventional works in Fukami *et al.* (2011) and Sasagawa (2014), we review the dynamical system based optical flow estimation.

2.1 The Optical Flow Equation

The gradient method for optical flow estimation is a technique in which estimations are made based on the assumption that brightness values do not vary while moving over infinitesimal time intervals (Horn and Schunck, 1981; Lucas and Kanade, 1981). Denoting the brightness value at time t and coordinates (x,y) by $I(x,y,t)$, they derive the following equation by assuming that brightness values remain unchanged after moving:

$$\frac{dI}{dt} = \frac{\partial I}{\partial x}u + \frac{\partial I}{\partial y}v + \frac{\partial I}{\partial t} = 0, \tag{1}$$

where u and v are the optical flows in the x and y directions, this relation is known as the optical flow equation. Sebe *et al.* (2009) regard the optical flow equation (1) as a dynamical system and apply Kalman filter to estimate the state of dynamical system, i.e., the optical flow.

2.2 Quasi-dense Estimation

Here we review the quasi-dense estimation method of Fukami *et al.* (2011). The quasi-dense estimation refers to an estimation method in which, rather than applying optical flow estimation to all pixels, it decimates the set of pixels and performs optical flow estimation on just the remaining subset. After optical flow estimation of the subset of pixels, an interpolation operator is applied to interpolate optical flow values, which are used to estimate brightness of all pixels. The quasi-dense estimation considers, optical flow estimation for a video image of height M and width N with L frames. The vectors q_u, q_v, whose components are the optical flows of each pixel $[u,v]^{\mathrm{T}}$, are defined as follows.

$$q_{u(k)} = \left[\begin{array}{cccc} u_{(1,1,k)} & u_{(1,2,k)} & \cdots & u_{(M,N,k)} \end{array}\right]^{\mathrm{T}}, \tag{2}$$

$$q_{u(k)} = \left[\begin{array}{cccc} v_{(1,1,k)} & v_{(1,2,k)} & \cdots & v_{(M,N,k)} \end{array}\right]^{\mathrm{T}}. \tag{3}$$

The decimated flows $\tilde{q}_u$, $\tilde{q}_v$ are given by

$$q_u = \mathcal{M}\tilde{q}_u, \tag{4}$$

$$q_v = \mathcal{M}\tilde{q}_v, \tag{5}$$

where $\mathcal{M}$ is an interpolating operator that interpolates $\tilde{q}_u$ and $\tilde{q}_v$ to obtain the flows q_u and q_v at all the pixels. Also, using the brightness I of each pixel, q_I is defined as follows:

$$q_{I(k)} = \left[\begin{array}{cccc} I_{(1,1,k)} & I_{(1,2,k)} & \cdots & I_{(M,N,k)} \end{array}\right]^{\mathrm{T}}. \tag{6}$$

Using these quantities, the state of dynamical system $q_{(k)}$ is defined as follows:

$$q_{(k)} = \left[\begin{array}{ccc} q_{I(k)}^{\mathrm{T}} & \tilde{q}_{u(k)}^{\mathrm{T}} & \tilde{q}_{v(k)}^{\mathrm{T}} \end{array}\right]^{\mathrm{T}}. \tag{7}$$

Also, $f(q_{(k)})$ is defined by

$$f(q_{(k)}) = \left[\begin{array}{c} q_{I(k)} - [\mathrm{diag}\{\mathcal{M}\tilde{q}_{u(k)}\}\mathcal{D}_x \\ \quad + \mathrm{diag}\{\mathcal{M}\tilde{q}_{v(k)}\}\mathcal{D}_y]q_{I(k)} \\ \tilde{q}_{u(k)} \\ \tilde{q}_{v(k)} \end{array}\right], \tag{8}$$

where $\mathcal{D}_x$, $\mathcal{D}_y$ are partial differential operators with respect to x, y. Using these equations, Fukami *et al.* (2011) regard optical flow equations of all pixels as a nonlinear dynamical system of the form

$$q_{(k+1)} = f(q_{(k)}), \tag{9}$$

$$I_{(k)} = Hq_{(k)}, \tag{10}$$

where $I_{(k)}, H$ are given by

$$I_{(k)} = \left[\begin{array}{cccc} I_{(1,1,k)} & I_{(1,2,k)} & \cdots & I_{(M,N,k)} \end{array}\right]^{\mathrm{T}}, \tag{11}$$

$$H = \left[\begin{array}{cc} E_{MN\times MN} & O_{MN\times 2L} \end{array}\right]. \tag{12}$$

The matrices $E_{m\times n}, O_{m\times n}$ are the $m\times n$ identity matrix and zero matrix, respectively.

2.3 Kalman Filter

Kalman filter is one of the most effective method for estimating the state of dynamical systems. Fukami *et al.* (2011) apply Kalman filter to the dynamical system (9), (10) to estimate the optical flow. For this purpose, they consider the following noise-added version of the model:

$$\begin{bmatrix} q_{I(k+1)} \\ \tilde{q}_{u(k+1)} \\ \tilde{q}_{v(k+1)} \end{bmatrix} = f(q_{(k)}) + \begin{bmatrix} \eta_{I(k)} \\ \eta_{u(k)} \\ \eta_{v(k)} \end{bmatrix}, \quad (13)$$

$$I_{(k)} = Hq_{(k)} + \zeta_{(k)}, \quad (14)$$

where $\eta_{(k)}$ denotes system noise, while $\zeta_{(k)}$ represents measurement noise; they take these to be Gaussian noise processes with covariance matrices $Q_{(k)}, R_{(k)}$. Also, the Jacobian $F_{(k)}$ of $f(q_{(k)})$ in equation (8) is

$$F_{(k)} = \begin{bmatrix} E + N(q_{(k)}) & J_u(q_{(k)}) & J_v(q_{(k)}) \\ O & E & O \\ O & O & E \end{bmatrix}, \quad (15)$$

where $N(q_{(k)}), J_u(q_{(k)}), J_v(q_{(k)})$ are given by

$$N(q_{(k)}) = -[\mathrm{diag}\{\mathcal{M}\tilde{q}_{u(k)}\}\mathcal{D}_x + \mathrm{diag}\{\mathcal{M}\tilde{q}_{v(k)}\}\mathcal{D}_y], \quad (16)$$

$$J_u(q_{(k)}) = -\mathrm{diag}\{\mathcal{D}_x q_{I(k)}\}\mathcal{M}, \quad (17)$$

$$J_v(q_{(k)}) = -\mathrm{diag}\{\mathcal{D}_y q_{I(k)}\}\mathcal{M}. \quad (18)$$

The procedures of extended Kalman filter time updates and measurement updates for the model of equations (13), (14), and (15) are as follows.
Time updates:

$$\hat{q}_{(k+1|k)} = f(\hat{q}_{(k|k)}), \quad (19)$$

$$\hat{F}_{(k)} = \begin{bmatrix} E + N(\hat{q}_{(k|k)}) & J_u(\hat{q}_{(k|k)}) & J_v(\hat{q}_{(k|k)}) \\ O & E & O \\ O & O & E \end{bmatrix}, \quad (20)$$

$$P_{(k+1|k)} = \hat{F}_{(k)} P_{(k|k)} \hat{F}^{\mathrm{T}}_{(k)} + Q_{(k)}. \quad (21)$$

Measurement updates:

$$\hat{q}_{(k+1|k+1)} = \hat{q}_{(k+1|k)} + K_{(k+1)}\{I_{(k+1)} - H\hat{q}_{(k+1|k)}\}, \quad (22)$$

$$P_{(k+1|k+1)} = P_{(k+1|k)} - K_{(k+1)} H P_{(k+1|k)}, \quad (23)$$

$$K_{(k+1)} = P_{(k+1|k)} H^{\mathrm{T}} \{H P_{(k+1|k)} H^{\mathrm{T}} + R_{(k)}\}^{-1}, \quad (24)$$

where $\hat{q}_{(m|k)}$ and $P_{(m|k)}$ are the estimate and the estimation error covariance matrix at time m from the state at time k, respectively. The estimation process proceeds by repeating the time update and measurement update for each time point.

2.4 Correcting Estimated Values using Measurement Residuals

In this subsection we review the method proposed in Sasagawa *et al.* (2013) for correcting estimated values by using measurement residuals. The estimation via extended Kalman filter may fail due to factors such as nonlinearities or flow boundaries. If the estimation fails, it does not subsequently recover, and for this reason the estimated values should be corrected. For cases in which they conclude that the estimation has failed, based on measurement residuals, they apply a reset procedure of the following form.

- The estimated brightness are reset to that of measured values.
- Because the flow value is unknown, the estimated flow values are reset to 0.
- For the covariance matrix, the diagonal elements are reset to large initial values to facilitate effective estimation; the off-diagonal elements are reset to 0 because they have no information about multivariable correlations.

2.5 Introduction of Artificial Diffusion Term

In this subsection, we review the diffusion term introduced by Sasagawa *et al.* (2013) . In methods (Sebe *et al.*, 2009; Fukami *et al.*, 2011), the dynamics of the optical flows are modeled as

$$\tilde{q}_{u(k+1)} = \tilde{q}_{u(k)}, \quad (25)$$

$$\tilde{q}_{v(k+1)} = \tilde{q}_{v(k)}. \quad (26)$$

These are augmented by a diffusion term capturing the smoothing effect of the estimation, as follows:

$$\tilde{q}_{u(k+1)} = D(\mathcal{D}_x^2 + \mathcal{D}_y^2)\tilde{q}_{u(k)}, \quad (27)$$

$$\tilde{q}_{v(k+1)} = D(\mathcal{D}_x^2 + \mathcal{D}_y^2)\tilde{q}_{v(k)}, \quad (28)$$

where D is a diffusion coefficient that determines the weight of the diffusion term. With the introduction of the diffusion term, equation (8) takes the form

$$f(q_{(k)}) = \begin{bmatrix} q_{I(k)} - [\mathrm{diag}\{\mathcal{M}\tilde{q}_{u(k)}\}\mathcal{D}_x + \mathrm{diag}\{\mathcal{M}\tilde{q}_{v(k)}\}\mathcal{D}_y] q_{I(k)} \\ D(\mathcal{D}_x^2 + \mathcal{D}_y^2)\tilde{q}_{u(k)} \\ D(\mathcal{D}_x^2 + \mathcal{D}_y^2)\tilde{q}_{v(k)} \end{bmatrix}. \quad (29)$$

Also, the Jacobian of equation (29) becomes

$$F_{(k)} = \begin{bmatrix} E + N(q_{(k)}) & J_u(q_{(k)}) & J_v(q_{(k)}) \\ O & D(\mathcal{D}_x^2 + \mathcal{D}_y^2) & O \\ O & O & D(\mathcal{D}_x^2 + \mathcal{D}_y^2) \end{bmatrix}. \quad (30)$$

2.6 Estimation Model with Brightness Constancy Corrections

In this subsection, we review an optical flow estimation model that takes into account the brightness constancy constraint in the neighborhood of flow boundaries (Sasagawa, 2014). When the flow becomes discontinuous due to occlusions or other factors, the brightness of objects that had previously been visible disappears, because it is obscured by some covering object. However, the optical flow equation used in the estimation model is based on the brightness constancy constraint and does not account for the possibility that brightness may be extinguished. For this reason, optical flow estimation is difficult in the neighborhood of flow boundaries. To address this difficulty, Sasagawa *et al.* (2013) reason that, in the event of an occlusion, brightness - being a constant quantity - flows in the perpendicular direction, and they add corrections to the optical flow equation describing the volume of the perpendicular brightness flow. These corrections should be applied only at flow boundaries, thus they construct the corrections to be proportional to the inner product of the flows boundary normal vector and the flow difference vector. However, because the normal vector to the flow boundary is unknown, they replace it with the brightness gradient vector, which they assume to point in the direction perpendicular to the boundary. Then the equation to be satisfied for each pixel takes the form shown in (33). The brightness gradient $\overrightarrow{\Delta I}$, which they use in place of the normal vector, and the difference vector are defined as follows.

$$\overrightarrow{\Delta I} = \begin{bmatrix} \frac{\partial I}{\partial x} \\ \frac{\partial I}{\partial y} \end{bmatrix}, \tag{31}$$

$$\begin{bmatrix} \Delta u \\ \Delta v \end{bmatrix} = \begin{bmatrix} \frac{\partial u}{\partial x} & \frac{\partial u}{\partial y} \\ \frac{\partial v}{\partial x} & \frac{\partial v}{\partial y} \end{bmatrix} \frac{\overrightarrow{\Delta I}}{\sqrt{I_x^2 + I_y^2}}. \tag{32}$$

They reason that the correction should be proportional to the inner product of the vectors (31) and (32), so the brightness constancy constraint is modified as follows.

$$\frac{\partial I}{\partial t} = -\left(\frac{\partial I}{\partial x}u + \frac{\partial I}{\partial y}v\right) - \overrightarrow{\Delta I}^{\mathrm{T}} \begin{bmatrix} \Delta u \\ \Delta v \end{bmatrix} z. \tag{33}$$

These corrections are large when large movements are made in the direction of the increasing brightness gradient. In the second term on the right-hand side of equation (33), they estimate only the quantity z by taking all other factors as proportionality constants. Using this model, they expect improved accuracy in the flow estimation near boundaries.

The above equation is a model for the equation that should hold for each pixel. They next present their model-description method for the image as a whole. They begin by adding z to the state of the estimation model.

$$q_{z(k)} = \begin{bmatrix} z_{(1,1,k)} & z_{(1,2,k)} & \cdots & z_{(M,N,k)} \end{bmatrix}^{\mathrm{T}}, \tag{34}$$

where they take $\tilde{q}_z$ to be

$$q_z = \mathcal{M}\tilde{q}_z. \tag{35}$$

As for the optical flows $\tilde{q}_u, \tilde{q}_v$, they apply decimation to q_z to guarantee observability. They apply the estimation procedure to the decimated vector $\tilde{q}_z$. Then the state $q_{(k)}$ may be defined as follows:

$$q_{(k)} = \begin{bmatrix} q_{I(k)}^{\mathrm{T}} & \tilde{q}_{u(k)}^{\mathrm{T}} & \tilde{q}_{v(k)}^{\mathrm{T}} & \tilde{q}_{z(k)}^{\mathrm{T}} \end{bmatrix}^{\mathrm{T}}. \tag{36}$$

Similar to the optical flows $\tilde{q}_u, \tilde{q}_v$, the dynamics of the perpendicular flow is modeled as

$$\tilde{q}_{z(k+1)} = \tilde{q}_{z(k)}. \tag{37}$$

Using equations (36) and (37), $f(q_{(k)})$ in equation (29) is modified as follows.

$$f(q_{(k)}) = \begin{bmatrix} \begin{pmatrix} q_{I(k)} - \{\mathrm{diag}\{\mathcal{M}\tilde{q}_{u(k)}\}\mathcal{D}_x \\ +\mathrm{diag}\{\mathcal{M}\tilde{q}_{v(k)}\}\mathcal{D}_y\}q_{I(k)} \\ -\mathrm{diag}\{\mathrm{diag}\{I_{x(k)}\}\Delta u_{(k)} \\ +\mathrm{diag}\{I_{y(k)}\}\Delta v_{(k)}\}\mathcal{M}\tilde{q}_{z(k)} \end{pmatrix} \\ D(\mathcal{D}_x^2 + \mathcal{D}_y^2)\tilde{q}_{u(k)} \\ D(\mathcal{D}_x^2 + \mathcal{D}_y^2)\tilde{q}_{v(k)} \\ \tilde{q}_{z(k)} \end{bmatrix}. \tag{38}$$

The quantities $I_{x(k)}, I_{y(k)}, \Delta u, \Delta v$ here are defined as follows.

$$\begin{aligned} I_{x(k)} &= \begin{bmatrix} \frac{\partial}{\partial x}I_{(1,1,k)} & \frac{\partial}{\partial x}I_{(1,2,k)} & \cdots & \frac{\partial}{\partial x}I_{(M,N,k)} \end{bmatrix}^{\mathrm{T}} \\ &= \mathcal{D}_x q_{I(k)}, \end{aligned} \tag{39}$$

$$\begin{aligned} I_{y(k)} &= \begin{bmatrix} \frac{\partial}{\partial y}I_{(1,1,k)} & \frac{\partial}{\partial y}I_{(1,2,k)} & \cdots & \frac{\partial}{\partial y}I_{(M,N,k)} \end{bmatrix}^{\mathrm{T}} \\ &= \mathcal{D}_y q_{I(k)}, \end{aligned} \tag{40}$$

$$\Delta u_{(k)} = \begin{bmatrix} \Delta u_{(1,1,k)} & \Delta u_{(1,2,k)} & \ldots & \Delta u_{(M,N,k)} \end{bmatrix}^{\mathrm{T}}, \tag{41}$$

$$\Delta v_{(k)} = \begin{bmatrix} \Delta v_{(1,1,k)} & \Delta v_{(1,2,k)} & \ldots & \Delta v_{(M,N,k)} \end{bmatrix}^{\mathrm{T}}. \tag{42}$$

The elements $\Delta u_{(x,y,k)}, \Delta v_{(x,y,k)}$ in equations (41) and (42) are the quantities $\Delta u, \Delta v$ of equation (32) for pixel (x,y) at time k. The calculation of the Jacobian is given in APPENDIX.

3 NEW PROPOSED METHOD

In this section we describe a new model that improves the model proposed in Sasagawa (2014).

3.1 Switching between Estimation Models based on Measurement Residuals

Using the model proposed in Sasagawa (2014), we successfully confirmed improved estimation accuracy in cases where the flow becomes discontinuous due to occlusions or other factors. However, their model also applied corrections to regions in which the flow was continuous; this caused an outflow of brightness and yielded the problematic result that the estimation accuracy of the model was inferior to that without the correction. To address this difficulty, we here propose a new model in which measurement residuals are used to switch between the model accounting for brightness constancy corrections and existing models. Our model modifies equation (33) as follows.

$$\frac{\partial I}{\partial t} = -\left(\frac{\partial I}{\partial x}u + \frac{\partial I}{\partial y}v\right) - \overrightarrow{\Delta I}^{\mathrm{T}} \left[\begin{array}{c} \Delta u \\ \Delta v \end{array}\right] Az. \quad (43)$$

The quantity A is defined by

$$A = \mathrm{diag}(a_{(1,1,k)}\ ,\ a_{(1,2,k)}\ ,\ \ldots\ ,\ a_{(M,N,k)}), \quad (44)$$

where,

$$a_{(i,j,k)} = \begin{cases} 1 & |(I_{(i,j,k)} - q_{I(k|k-1)}| \geq \tau), \\ 0 & |(I_{(i,j,k)} - q_{I(k|k-1)}| < \tau). \end{cases} \quad (45)$$

In equation (45), $I_{(i,j,k)} - q_{I(k|k-1)}$ is the measurement residual and τ is a threshold value. The function $a(i,j,k)$ is a step function taking the value 1 if the measurement residual exceeds the threshold, and 0 otherwise. This ensures that, in a region of flow discontinuities, the correction represented by the second term of equation (43) is present, while this term is removed in regions of continuous flow, and ensures that no correction is applied. Equation (33) has the flaw that the correction term is present even in regions where there is no occlusion and the flow is continuous, and thus results in an outflow of brightness that degrades the estimation accuracy. In contrast, equation (43) uses measurement residuals and a step function to ensure that the model that attempts to apply brightness constancy corrections is not used in regions where the flow is continuous, and thus promises improved estimation accuracy. Because we modified equation (33) according to (43), $f(q_{(k)})$ in equation (38) is modified to

$$f_A(q_{(k)}) = \left[\begin{array}{c} \left(\begin{array}{c} q_{I(k)} - \{\mathrm{diag}\{\mathcal{M}\tilde{q}_{u(k)}\}\mathcal{D}_x \\ +\mathrm{diag}\{\mathcal{M}\tilde{q}_{v(k)}\}\mathcal{D}_y\}q_{I(k)} \\ -\mathrm{diag}\{\mathrm{diag}\{I_{x(k)}\}\Delta u_{(k)} \\ +\mathrm{diag}\{I_{y(k)}\}\Delta v_{(k)}\}A\mathcal{M}\tilde{q}_{z(k)} \end{array}\right) \\ D(\mathcal{D}_x^2 + \mathcal{D}_y^2)\tilde{q}_{u(k)} \\ D(\mathcal{D}_x^2 + \mathcal{D}_y^2)\tilde{q}_{v(k)} \\ \tilde{q}_{z(k)} \end{array}\right]. \quad (46)$$

The Jacobian of (46) is given in APPENDIX.

4 NUMERICAL EXPERIMENTS

In this section we conduct numerical experiments to test the efficacy of the model proposed in Section 3.1.

4.1 Description of Experiments

The video images used in these numerical experiments are taken from the sleeping2 sample in the MPI Sintel benchmark (Butler *et al.*, 2012) . For our tests, we extract the regions delineated by white frames in Figures 1 and 2. We performed estimation on a 60 60 pixel region. To track flow boundaries through all frames, we displace the test region by 1 pixel per frame in the imaging direction (Brox *et al.*, 2004). The covariance matrices are set to

$$\begin{aligned} Q_{I(k)} &= 0.001E, && (47)\\ Q_{u(k)} &= Q_{v(k)} && (48)\\ &= 0.4E, && (49)\\ R_{(k)} &= 0.1E. && (50) \end{aligned}$$

We set the measurement residual τ in equation (45) to 10. For numerical integration we used the 4th-order Runge-Kutta method with 4 time steps per frame. We used the endpoint error to assess the optical flow estimation accuracy for each pixel. The endpoint error is the distance between the tips of the estimated flow vector $\tilde{U}$ and the actual flow vector U and may be determined by using equation (51).

$$\sqrt{(\tilde{U} - U)^{\mathrm{T}}(\tilde{U} - U)}. \quad (51)$$

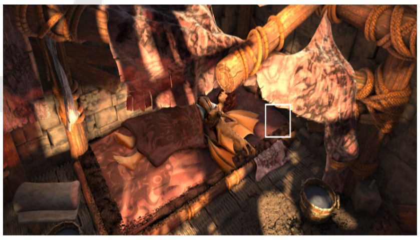

Figure 1: Frame 1 of video image containing a boundary.

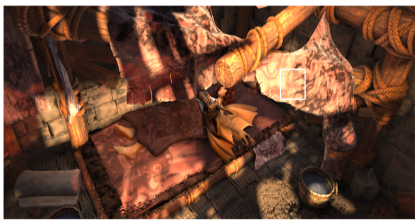

Figure 2: Frame 1 of video image not containing a boundary.

4.2 Investigating the Difference of Estimate Accuracy Among Three Models

We investigate the difference of the estimate accuracy among the model proposed in Section 3, Fukami model and the model in Sasagawa (2014) by numerical experimants. Here, Fukami model is that Fukami *et al.* (2011) includes correcting estimated values using measurement residuals and diffusion term. Figures 3 and 4 show the mean endpoint error for image frames containing boundaries and not containing boundaries, respectively. The mean endpoint errors for all frames are listed in Table 1.

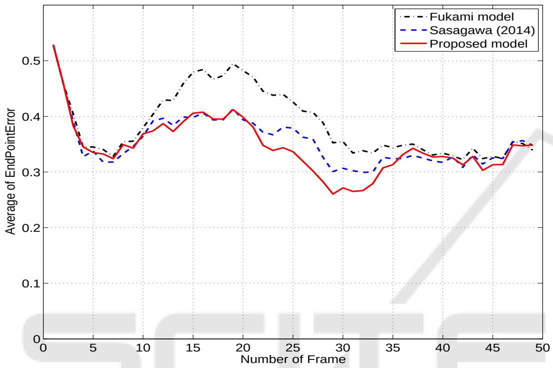

Figure 3: Mean endpoint error for each frame of the boundary containing images.

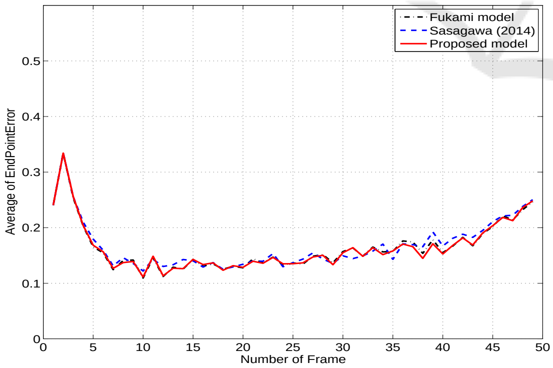

Figure 4: Mean endpoint error for each frame of the non boundary containing images.

Table 1: Mean endpoint errors for all frames.

	Images containing boundary	Images not containing boundary
Fukami model	0.3875	0.1642
Sasagawa (2014)	0.3549	0.1674
Proposed model	0.3454	0.1636

Figure 5 shows the estimation frame containing a boundary. For this image, Figures 6 and 7 show the endpoint error of frame 30 for Sasagawa (2014) and the proposed model, respectively. Next, Figure 8 shows the estimation frame that does not contain a boundary. For this image, the endpoint error of frame 40 obtained with Sasagawa (2014) and the proposed model are shown in Figures 9 and 10, respectively.

Figure 5: Estimation region for frame 30 of the image containing a boundary.

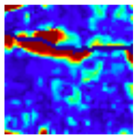

Figure 6: Endpoint error for image of Figure 5 (frame 30, Sasagawa (2014)).

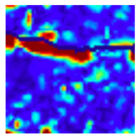

Figure 7: Endpoint error for image of Figure 5 (frame 30, proposed model).

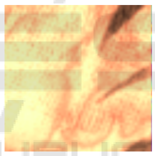

Figure 8: Estimation region for frame 40 of the image not containing a boundary.

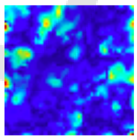

Figure 9: Endpoint error for image of Figure 8 (frame 40, Sasagawa (2014)).

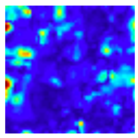

Figure 10: Endpoint error for image of Figure 8 (frame 40, proposed model).

For the images containing a boundary, Figures 11 and 12 show values of the correction term z determined by Sasagawa (2014) and the proposed model, respectively. For the images not containing a boundary, Figures 13 and 14 show values of the correction term z determined by Sasagawa (2014) and the proposed model, respectively.

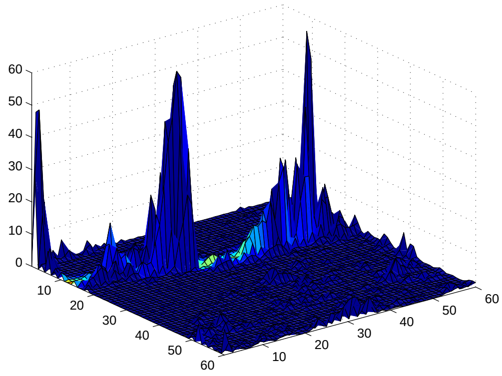

Figure 11: Correction term z determined by Sasagawa (2014) for frame 30 of the image containing a boundary.

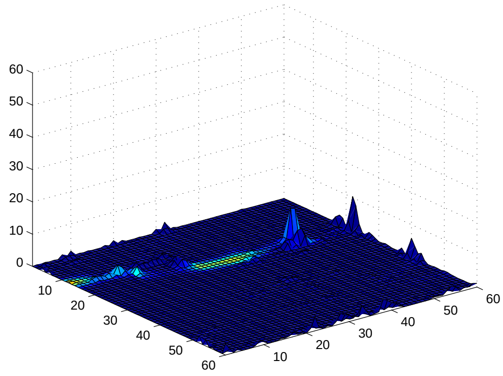

Figure 12: Correction term z determined by the proposed model for frame 30 of the image containing a boundary.

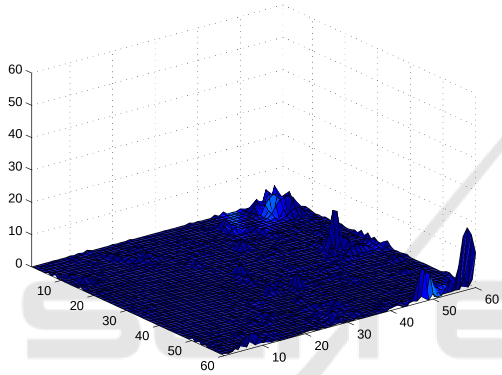

Figure 13: Correction term z determined by Sasagawa (2014) for frame 40 of the image not containing a boundary.

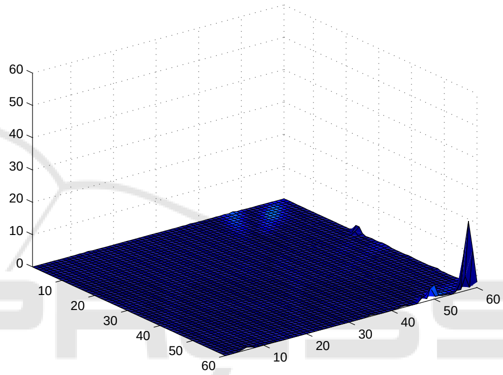

Figure 14: Correction term z determined by the proposed model for frame 40 of the image not containing a boundary.

5 DISCUSSION

Our numerical experiments to compare the estimation accuracy of Sasagawa (2014) and the proposed model confirm the efficacy of our proposed model. For estimation of the image containing a boundary, Figure 3 shows that the estimation accuracy of the proposed model is superior to that of Sasagawa (2014). As we see in Figures 6 and 7, this is because the measurement residuals are small, whereas the model proposed in this paper does not apply corrections in regions of continuous flow, and so yield improved estimation accuracy. From Figure 4 we see that the proposed model also achieves superior estimation accuracy when estimating regions that do not contain boundaries. From Figures 12 and 14 we see that the proposed model yields a value of 0 for the correction term z in regions where the flow is continuous. This confirms that, in regions not containing boundaries, our proposed model correctly switches to the model that ignores corrections.

At the end of this section, we briefly give a comment on the computational cost. The examples are carried out by MATLAB (Release 2011a) on a PC (core i7-4790K, 4.00GHz with 16GB RAM). We use 4 cores to carry out the example with the proposed method, and it takes about 40.3 [sec]. As the extended Kalman filter calculates a huge error covariance matrix, enormous computational cost is required. To reduce the computational cost, mathematical tools used in data assimilation, e.g. the ensemble Kalman filter, might be applicable. Reducing the computational cost is one of our important future works.

6 CONCLUSIONS

Our numerical experiments confirm the effectiveness of our proposed model. In the proposal model, we switched between two models: one that accounts for corrections to the brightness constancy constraint and one that does not use measurement residuals. This ensures that corrections are not applied in regions where the flow is continuous, and so the estimation accuracy is superior to that of Sasagawa (2014). In addition, a step function is used to switch between models based on measurement residuals in this model. In future work, we plan to replace this with a sigmoid or other nonlinear function to achieve further improvements in estimation accuracy. Furthermore, the information of measurement residual can be used to modify the diffusion coefficient. This modification realizes the nonlinear diffusion used in Brox and Weicket (2002). This is also our future work.

REFERENCES

Brox, T., Bruhn, A., Pepenberg, N., and Weickert, J. (2004). High accuracy optical flow estimation based on a theory for warping. *European Conference on Computer Vision (ECCV)*, pages 25–36.

Butler, D. J., Wulff, J., Stanley, G. B., and Black, M. J. (2012). A naturalistic open source movie for optical flow evaluation. *Conf. on Computer Vision (ECCV)*, pages 611–625.

Fukami, T., Enokida, S., Sebe, N., and Nobuyama, E. (2011). Quasi-dense optical flow estimation based on dynamical system models. *SICE Annual Conference*, pages 802–811.

Horn, B. K. P. and Schunck, B. G. (1981). Determining optical flow. *Artificial Intelligence*, pages 185–203.

Lucas, K. and Kanade, T. (1981). An interactive image registration techniques with an application to stereo vision. In *Proceedings of 7th IJCAL*, pages 674–679.

Sasagawa, T. (2014). Optical flow estimation accuracy improvement in the flow near the boundary. *Kyushu Institute of Technology Graduate School of master's thesis*.

Sasagawa, T., Sebe, N., Enokida, S., Nobuyama, E., and Fukami, T. (2013). Improvement of the accuracy of the optical flow estimation by simultaneous estimation of flow boundary. *The 32nd SICE Kyushu Branch Annual Conference*, pages 151–154.

Sebe, N., Nobuyama, E., and Enokida, S. (2009). Optical flow estimation method in the moving image by the dynamic systems theory approach. *The 38th Symposium on Control Theory*, pages 357–362.

Thomas Brox, J. W. (2002). Nonlinear matrix diffusion for optic flow estimation. *Pattern Recognition (Proc. DAGM)*, pages 446–453.

APPENDIX

A.1. Jacobian of Sasagawa's Model

The Jacobian $F_{(k)}$ of (38) is given.

$$F_{(k)} = \left[\begin{array}{cccc} E+N(q_{(k)}) & J_u(q_{(k)}) & J_v(q_{(k)}) - \mathrm{diag}\{g_{v(k)}\}\mathcal{M} & J_z(q_{(k)}) \\ -\mathrm{diag}\{g_{I(k)}\} & -\mathrm{diag}\{g_{u(k)}\}\mathcal{M} & O & O \\ O & D(\mathcal{D}_x^2+\mathcal{D}_y^2) & D(\mathcal{D}_x^2+\mathcal{D}_y^2) & O \\ O & O & O & E \end{array} \right], \quad (52)$$

where

$$J_z(q_{(k)}) = -\left[\begin{array}{c} \mathrm{diag}\{\mathrm{diag}\{I_{x(k)}\}\Delta u_{(k)} \\ +\,\mathrm{diag}\{I_{y(k)}\}\Delta v_{(k)}\} \end{array} \right]\mathcal{M}. \quad (53)$$

The correction term g is defined by

$$g = \overrightarrow{\Delta I}^{\mathrm{T}} \left[\begin{array}{c} \Delta u \\ \Delta v \end{array} \right] z. \quad (54)$$

The notation $g(x,y,k)$ is used to denote the value of equation (54) at pixel (x,y) and time k. The quantities $g_{I(k)}, g_{u(k)}, g_{v(k)}$ in equation (52) may be expressed as follows in terms of partial differentials of q_I, q_u, q_v.

$$g_{I(k)} = \left[\begin{array}{ccc} \frac{\partial}{\partial I} g_{(1,1,k)} & \frac{\partial}{\partial I} g_{(1,2,k)} & \cdots & \frac{\partial}{\partial I} g_{(M,N,k)} \end{array} \right]^{\mathrm{T}}, \quad (55)$$

$$g_{u(k)} = \left[\begin{array}{ccc} \frac{\partial}{\partial u} g_{(1,1,k)} & \frac{\partial}{\partial u} g_{(1,2,k)} & \cdots & \frac{\partial}{\partial u} g_{(M,N,k)} \end{array} \right]^{\mathrm{T}}, \quad (56)$$

$$g_{v(k)} = \left[\begin{array}{ccc} \frac{\partial}{\partial v} g_{(1,1,k)} & \frac{\partial}{\partial v} g_{(1,2,k)} & \cdots & \frac{\partial}{\partial v} g_{(M,N,k)} \end{array} \right]^{\mathrm{T}}. \quad (57)$$

Also, $g_{I_x(k)}, g_{I_y(k)}, g_{u_x(k)}, g_{u_y(k)}, g_{v_x(k)}, g_{v_y(k)}$ are given by

$$g_{I_x(k)} = \left[\frac{\partial}{\partial I_x} g_{(1,1,k)} \; \frac{\partial}{\partial I_x} g_{(1,2,k)} \cdots \frac{\partial}{\partial I_x} g_{(M,N,k)} \right]^{\mathrm{T}}, \quad (58)$$

$$g_{I_y(k)} = \left[\frac{\partial}{\partial I_y} g_{(1,1,k)} \; \frac{\partial}{\partial I_y} g_{(1,2,k)} \cdots \frac{\partial}{\partial I_y} g_{(M,N,k)} \right]^{\mathrm{T}}, \quad (59)$$

$$g_{u_x(k)} = \left[\frac{\partial}{\partial u_x} g_{(1,1,k)} \; \frac{\partial}{\partial u_x} g_{(1,2,k)} \cdots \frac{\partial}{\partial u_x} g_{(M,N,k)} \right]^{\mathrm{T}}, \quad (60)$$

$$g_{u_y(k)} = \left[\frac{\partial}{\partial u_y} g_{(1,1,k)} \; \frac{\partial}{\partial u_y} g_{(1,2,k)} \cdots \frac{\partial}{\partial u_y} g_{(M,N,k)} \right]^{\mathrm{T}}, \quad (61)$$

$$g_{v_x(k)} = \left[\frac{\partial}{\partial v_x} g_{(1,1,k)} \; \frac{\partial}{\partial v_x} g_{(1,2,k)} \cdots \frac{\partial}{\partial v_x} g_{(M,N,k)} \right]^{\mathrm{T}}, \quad (62)$$

$$g_{v_y(k)} = \left[\frac{\partial}{\partial v_y} g_{(1,1,k)} \; \frac{\partial}{\partial v_y} g_{(1,2,k)} \cdots \frac{\partial}{\partial v_y} g_{(M,N,k)} \right]^{\mathrm{T}}. \quad (63)$$

The partial differentials of g in equation (54) are given by

$$\frac{\partial g}{\partial I} = \frac{\partial g}{\partial I_x}\frac{\partial I_x}{\partial I} + \frac{\partial g}{\partial I_y}\frac{\partial I_y}{\partial I}, \quad (64)$$

$$\frac{\partial g}{\partial u} = \frac{\partial g}{\partial u_x}\frac{\partial u_x}{\partial u} + \frac{\partial g}{\partial u_y}\frac{\partial u_y}{\partial u}, \quad (65)$$

$$\frac{\partial g}{\partial v} = \frac{\partial g}{\partial v_x}\frac{\partial v_x}{\partial v} + \frac{\partial g}{\partial v_y}\frac{\partial v_y}{\partial v}. \quad (66)$$

Also,

$$\begin{aligned}\frac{\partial g}{\partial I_x} &= \{I_x^3 u_x + I_y^3(u_y + v_x) \\ &\quad + I_x I_y^2(2u_x - v_y)\}(I_x^2 + I_y^2)^{-\frac{3}{2}} z, \quad (67)\\ \frac{\partial g}{\partial I_y} &= \{I_y^3 v_y + I_x^3(u_y + v_x) \\ &\quad + I_x^2 I_y(2v_y - u_x)\}(I_x^2 + I_y^2)^{-\frac{3}{2}} z, \quad (68)\\ \frac{\partial g}{\partial u_x} &= I_x^2(I_x^2 + I_y^2)^{-\frac{1}{2}} z, \quad (69)\end{aligned}$$

$$\begin{aligned}\frac{\partial g}{\partial u_y} &= I_x I_y(I_x^2 + I_y^2)^{-\frac{1}{2}} z, \quad (70)\\ \frac{\partial g}{\partial v_x} &= I_x I_y(I_x^2 + I_y^2)^{-\frac{1}{2}} z, \quad (71)\\ \frac{\partial g}{\partial v_y} &= I_y^2(I_x^2 + I_y^2)^{-\frac{1}{2}} z. \quad (72)\end{aligned}$$

From equations (64), (65), (66), the quantities $g_{I_{(k)}}, g_{u_{(k)}}, g_{v_{(k)}}$ in equations (55), (56), (57) may be computed as follows:

$$g_{I(k)} = \left[\mathrm{diag}\{g_{I_x(k)}\}\mathcal{D}_x + \mathrm{diag}\{g_{I_y(k)}\}\mathcal{D}_y\right] q_{I(k)}, \quad (73)$$

$$g_{u(k)} = \left[\mathrm{diag}\{g_{u_x(k)}\}\mathcal{D}_x + \mathrm{diag}\{g_{u_y(k)}\}\mathcal{D}_y\right] q_{u(k)}, \quad (74)$$

$$g_{v(k)} = \left[\mathrm{diag}\{g_{v_x(k)}\}\mathcal{D}_x + \mathrm{diag}\{g_{v_y(k)}\}\mathcal{D}_y\right] q_{v(k)}. \quad (75)$$

A.2. Jacobian of the Proposed Model

The Jacobian $F_{(k)}$ of (46) is given as follows:

$$F_{A(k)} = \begin{bmatrix} E + N(q_{(k)}) & J_u(q_{(k)}) & J_v(q_{(k)}) - \mathrm{diag}\{g_{Av(k)}\}\mathcal{M} & J_{Az}(q_{(k)}) \\ -\mathrm{diag}\{g_{AI(k)}\} & -\mathrm{diag}\{g_{Au(k)}\}\mathcal{M} & O & O \\ O & D(\mathcal{D}_x^2 + \mathcal{D}_y^2) & D(\mathcal{D}_x^2 + \mathcal{D}_y^2) & O \\ O & O & O & E \\ O & O & & \end{bmatrix}, \quad (76)$$

where

$$J_{Az}(q_{(k)}) = -\begin{bmatrix} \mathrm{diag}\{\mathrm{diag}\{I_{x(k)}\}\Delta u_{(k)} \\ +\,\mathrm{diag}\{I_{y(k)}\}\Delta v_{(k)}\} \end{bmatrix} A\mathcal{M}. \quad (77)$$

Also, the correction term g_A is defined as follows:

$$g_A = \overrightarrow{\Delta I}^{\mathrm{T}} \begin{bmatrix} \Delta u \\ \Delta v \end{bmatrix} Az. \quad (78)$$

We denote by $g_{A(x,y,k)}$ the value of equation (78) for pixel (x,y) at time k; The quantities $g_{AI(k)}, g_{Au(k)}, g_{Av(k)}$ in equation (76) are defined as follows:

$$g_{AI(k)} = Ag_{I(k)}, \quad (79)$$

$$g_{Au(k)} = Ag_{u(k)}, \quad (80)$$

$$g_{Av(k)} = Ag_{v(k)}. \quad (81)$$